Fluctuation and Noise Letters
Vol. 0, No. 0 (2005) 000–000

Stokes' Drift and Hypersensitive Response with Dichotomous Markov Noise

I. BENA*
Department of Theoretical Physics, University of Geneva
CH-1211, Geneva 4, Switzerland
**Ioana.Bena@physics.unige.ch*

R. KAWAI
Department of Physics, University of Alabama at Birmingham
Birmingham, AL 35294

C. VAN DEN BROECK
Limburgs Universitair Centrum
B-3590 Diepenbeek, Belgium

KATJA LINDENBERG
Department of Chemistry and Biochemistry 0340 and Institute for Nonlinear Science,
University of California, San Diego
9500 Gilman Drive, La Jolla, CA 92093-0340

Received (received date)
Revised (revised date)
Accepted (accepted date)

Stochastic Stokes' drift and hypersensitive transport driven by dichotomous noise are theoretically investigated. Explicit mathematical expressions for the asymptotic probability density and drift velocity are derived including the situation in which particles cross unstable fixed points. The results are confirmed by numerical simulations.

Keywords: Dichotomous noise, unstable fixed point, Stokes' drift, hypersensitive response, rocking ratchet, Brownian motor

1. Introduction

The response of a Brownian particle to an external force is one of the paradigms of statistical mechanics. Brownian motion is usually described as a Wiener process and a full mathematical analysis is possible based on the solution of the corresponding Fokker-Planck equation. However, a genuine Gaussian white noise does not exist in real systems, and the importance of other types of noises has long been clear. Such noises have been studied in great detail in zero-dimensional systems, and their

specific properties are known to have a profound influence on the behavior of these systems [1, 2]. The effect of the color of the noise on noise-induced transitions continues to be documented [3, 4, 5], and has been found to be quite dramatic since it can alter the type of transition and lead to new re-entrance phenomena. Other noise-induced effects have also been found to be sensitive to the correlation time of the noise, e.g., stochastic resonance [6], synchronization [7], and transport in Brownian ratchets [5].

The two most commonly discussed examples of colored noise are the Ornstein-Uhlenbeck process and the dichotomous Markov process [8]. The latter has the great advantage that analytic results can often be derived. Nevertheless an essential technical difficulty restricts almost all the results obtained in the past to dynamics with no fixed points, or exclusively with stable fixed points, see for example [2]. We have recently made progress toward overcoming the technical difficulty that appears in the presence of unstable fixed points by identifying the source of spurious divergences that arise in the usual analytic approaches to the problem [9, 10], and are now in the position to consider these cases as well.

The purpose of this paper is to apply the general analytic procedure we developed in Ref. [10] to two different stochastic phenomena driven by dichotomous Markov noise, namely Stokes' drift [11] and hypersensitive transport [12, 13]. Section 2 deals with Stokes' drift as a rocking ratchet problem and Sec. 3 with hypersensitive transport. A short summary is presented in Sec. 4. Some of the lengthy calculations have been collected in the Appendices. All the analytical results are supported by numerical simulations of the corresponding dynamics of an ensemble of 20000 particles, with random initial positions, sampled at 100 different times in order to build up the histogram of the stationary probability density and, from it, to compute the value of the asymptotic mean velocity.

2. Stochastic Stokes' Drift as A Rocking Ratchet

A longitudinal wave traveling through a viscous fluid imparts a net drift to the suspended particles, an effect known as Stokes' drift. The deterministic effect (that does not account for the stochastic fluctuations or perturbations in the system) has been extensively studied in various practical contexts ranging from the motion of tracers in meteorology and oceanography [14] to doping impurities in crystal growth [15]. The deterministic drift has a simple intuitive explanation, namely that the suspended particle spends a longer time in the regions of the wave-train where the force due to the wave acts in the direction of the propagation of the wave than the time it spends in those regions where the force acts in the opposite direction. Therefore, the particle is driven on average in the direction of wave propagation. As a simple clarifying example [16], consider the dynamics of an overdamped particle forced by a traveling square wave with velocity v and wavelength L,

$$\dot{x} = f(x - vt), \tag{1}$$

where $x(t)$ is the position of the overdamped particle at time t, and f is the periodic forcing due to the longitudinal wave traveling at the speed v and of wavelength L. Suppose that the particle is entrained with a force $f = bv$ when in a crest part of the wave, and $f = -bv$ when in a trough part. The time spent in a crest part,

$L/[2(1-b)v]$, is larger than in the though part, $L/[2(1+b)v]$, resulting in a net deterministic drift velocity $v_0 = b^2\, v$ of the particle.

Recent studies [11, 16, 17] show the importance of stochastic effects on Stokes' drift. The thermal diffusion of the dragged particles, as well as the application of an external colored noise, can markedly modify the direction and magnitude of the Stokes' drift velocity. Furthermore, it has been shown that such a stochastic Stokes' drift is equivalent to another paradigm of Brownian motors, the rocking ratchet [18]. In this scenario, the systematic motion acquired under the influence of an alternating zero-average stochastic force revolves essentially around the asymmetry of the nonlinear response in the presence of a steady asymmetric potential [20]. This mathematical equivalence between stochastic Stokes' drift and Brownian motors hints at various potential applications of Stokes' drift, for instance, transport by capillary waves, storage of light in quantum wells, single-electron transport in one-dimensional channels, optical tweezing of colloidal particles, and diffusion of dislocations in solids, as noted in [19] and references therein.

In this paper we show, with an analytically solvable model, that the characteristics of the one-dimensional stochastic Stokes' drift are quite complex, and that various interesting phenomena are induced, including enhancement of the deterministic drift and current reversal, when the particles are subjected to an additive colored noise, specifically, a dichotomous noise. The starting point is the following stochastic equation with an additive symmetric dichotomous perturbation:

$$\dot{x} = f(x - vt) + A\xi(t). \tag{2}$$

The dichotomous perturbation has an amplitude A and the stochastic variable $\xi(t)$ takes on the values ± 1 with a transition rate k. It is appropriate to assume, on physical grounds, that the particle cannot move faster than the wave and thus $f(y) < v$ for all y. The quantity of interest is the asymptotic drift velocity, $\langle \dot{x} \rangle = \lim_{t\to\infty} \langle x(t) \rangle / t$, where the brackets indicate an average over the realizations of the dichotomous noise. Introducing a new variable $y(t) = x(t) - vt$, one can rewrite Eq. (2) as

$$\dot{y} = F(y) + A\xi(t), \tag{3}$$

with a time-independent periodic force, $F(y + L) = F(y) = f(y) - v < 0$. Equation (3) is a variant of the general stochastic differential equations solved in [9, 10], with a dichotomous force $F(y) \pm A$.

The behavior of the system, and the corresponding solution of the associated master equation for the probability density, depend on whether or not there are unstable fixed points in the "$\pm$" dynamics. We present below the results for the two simplest cases, namely, one with no fixed points (in Sec. 2.1), and the other with two fixed points in the "+" dynamics and no fixed points in the "$-$" dynamics (in Sec. 2.2).

2.1. *Systems with no fixed points*

When $A > \max |F(y)|$ or $0 < A < \min |F(y)|$, there are no fixed points. Then one obtains the following expressions (see Eqs. (7) and (8) in Ref. [10]) for the

asymptotic probability density,

$$P(y) = \frac{\langle \dot{y} \rangle}{L} \left\{ \left[F^2(y) - A^2 \right] \left[\exp\left(\int_0^L dz \frac{2kF(z)}{F^2(z) - A^2} \right) - 1 \right] \right\}^{-1} \times \int_y^{y+L} dz \left[F'(z) + 2k \right] \exp\left(- \int_z^y dw \frac{2kF(w)}{F^2(w) - A^2} \right), \tag{4}$$

and for the asymptotic mean velocity,

$$\begin{aligned} \langle \dot{x} \rangle &= v + \langle \dot{y} \rangle \\ &= v + L \left[\exp\left(\int_0^L dz \, \frac{2kF(z)}{F^2(z) - A^2} \right) - 1 \right] \\ &\quad \times \left\{ \int_0^L dy \int_y^{y+L} dz \frac{F'(z) + 2k}{F^2(y) - A^2} \exp\left(- \int_z^y dw \, \frac{2kF(w)}{F^2(w) - A^2} \right) \right\}^{-1}. \end{aligned} \tag{5}$$

Here $F'(y)$ denotes the derivative with respect to y. The detailed analysis of these results, including the possibility of current reversal, were already discussed in Ref. [11].

2.2. *Systems with asymptotic fixed points*

If the amplitude of the noise lies in the intermediate regime $\min |F(y)| < A < \max |F(y)|$, then the "+" dynamics has at least one pair of fixed points in $[0, L)$. We consider here the simplest case in which there is only one pair of fixed points, namely, a stable fixed point y_1 with $F'(y_1) < 0$, and an unstable fixed point $y_2 > y_1$ with $F'(y_2) > 0$. However, systems with several pairs of fixed points can be treated in the same way. According to the general discussion in Section III.B of Ref. [10], the probability density in the interval $[y_1, y_1 + L)$ is given by

$$P(y) = \frac{\langle \dot{y} \rangle}{L} \frac{1}{|F^2(y) - A^2|} \int_{y_2}^y dz \, \mathrm{sgn}[F^2(z) - A^2][F'(z) + 2k] \times \exp\left(- \int_z^y dw \, \frac{2kF(w)}{F^2(w) - A^2} \right). \tag{6}$$

Equation (6) is continuous at the unstable fixed point y_2, with

$$\lim_{y \nearrow y_2} P(y) = \lim_{y \searrow y_2} P(y) = - \frac{\langle \dot{y} \rangle}{L} \frac{2k + F'(y_2)}{2A \left[k + F'(y_2) \right]}. \tag{7}$$

Noting that $F'(y_2) > 0$ and $P(y_2) \geqslant 0$, $\langle \dot{y} \rangle$ is necessarily zero or negative. This immediately suggests that the direction of the net drift $\langle \dot{x} \rangle = \langle \dot{y} \rangle + v$ can be reversed by varying the amplitude A or the transition rate k of the dichotomous perturbation. The details of this current reversal phenomenon are discussed in a later section. At the stable fixed point y_1 the probability density is continuous only for $k/|F'(y_1)| > 1$ and its value is

$$\lim_{y \searrow y_1} P(y) = \lim_{y \nearrow y_1} P(y) = - \frac{\langle \dot{y} \rangle}{L} \frac{2k - |F'(y_1)|}{2A \left[k - |F'(y_1)| \right]}. \tag{8}$$

For $k/|F'(y_1)| \leqslant 1$, $P(y)$ is divergent at y_1 but integrable.

The corresponding mean velocity is given by

$$\begin{aligned}\langle \dot{x} \rangle =& v + L \left\{ \int_{y_1}^{y_1+L} dy \int_{y_2}^{y} dz \frac{\operatorname{sgn}\left[F^2(z) - A^2\right] \left[F'(z) + 2k\right]}{|F^2(y) - A^2|} \right. \\ & \left. \times \exp\left(- \int_z^y dw \, \frac{2kF(w)}{F^2(w) - A^2} \right) \right\}^{-1} .\end{aligned} \tag{9}$$

Note that if several waves are present, their contributions are not additive due to the highly nonlinear dependence of $\langle \dot{x} \rangle$ on F. This seems to be a general feature of the stochastic Stokes' drift [11, 16, 17], contrary to the deterministic drift.

2.3. *The square wave*

The above results are valid for an arbitrary form of the wave $F(y)$, provided that the obvious necessary differentiability and integrability conditions are fulfilled. However, due to the multiple integrals in Eqs. (6) and (9), further analytic investigation without a simple form of $F(y)$ is difficult. Following our previous work [11, 10], we use a piecewise linear wave

$$F(y) = \begin{cases} -(1-b)v & \text{for } y \in [0, L/2 - 2l) \\ -(1-b)v - \dfrac{bv}{l}(y - L/2 + 2l) & \text{for } y \in [L/2 - 2l, L/2) \\ -(1+b)v & \text{for } y \in [L/2, L - 2l) \\ -(1+b)v + \dfrac{bv}{l}(y - L + 2l) & \text{for } y \in [L - 2l, L) \end{cases} , \tag{10}$$

with $0 < b < 1$, and $F(y + L) = F(y)$. Although the analytic treatment is possible, the general solutions are still rather complicated, and the results are relegated to Appendix A. We focus here on the results in the limit of a square wave $l \to 0$, for which

$$F(y) = \begin{cases} -F_- \equiv -(1-b)v & \text{for } y \in [0, L/2) \\ -F_+ \equiv -(1+b)v & \text{for } y \in [L/2, L) \end{cases} . \tag{11}$$

It should be noted that this limit is singular and must be handled with some care.

From Eq. (4) one obtains the probability density for $A > F_+$ or $0 < A < F_-$,

$$P(y) = \begin{cases} \dfrac{\langle \dot{y} \rangle}{L} \left[\dfrac{2A^2 bv \left(1 - e^{\phi_2}\right) e^{2\phi_1 y/L}}{F_+ F_- (F_-^2 - A^2) \left(e^{\phi_1 + \phi_2} - 1\right)} - \dfrac{1}{F_-} \right] & \text{for } y \in [0,\, L/2) \\ \dfrac{\langle \dot{y} \rangle}{L} \left[\dfrac{2A^2 bv \left(1 - e^{\phi_1}\right) e^{\phi_2 (2y/L - 1)}}{F_+ F_- (A^2 - F_+^2) \left(e^{\phi_1 + \phi_2} - 1\right)} - \dfrac{1}{F_+} \right] & \text{for } y \in [L/2,\, L) \end{cases} , \tag{12}$$

where

$$\phi_{1,2} = \frac{LkF_\mp}{F_\mp^2 - A^2}. \tag{13}$$

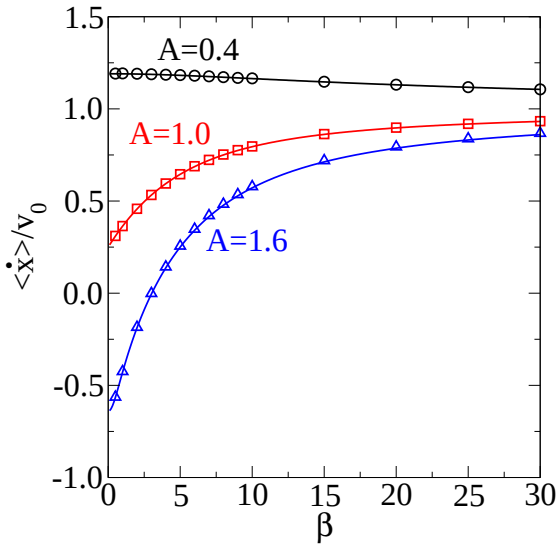

Fig 1. The asymptotic Stokes' drift velocity (normalized by its deterministic value $v_0 = b^2 v$) as a function of normalized transition rate $\beta = 2kvL/A^2$ for three different cases. The symbols are the results of numerical simulations. *Circles:* $A = 0.4 < F_-$ (no fixed point); *squares:* $F_- < A = 1.0 < F_+$ (two fixed points); *triangles:* $A = 1.6 > F_+$ (no fixed point). The solid lines indicate the results of theory. The values of the other parameters are $v = 1$, $b = 0.5$, and $L = 1$. The direction of the drift velocity remains the same for $A = 0.4$ and $A = 1.0$, but is reversed for $A = 1.6$.

Integrating Eq. (6), we find the probability for $F_- < A < F_+$,

$$P(y) = \begin{cases} \dfrac{\langle \dot{y} \rangle}{L} \left[\dfrac{(1 - e^{\phi_1})(F_- - A)}{kF_-} \delta_-(y - L/2) \right. & \\ \left. \quad + \dfrac{A\, e^{2\phi_1 y/L}}{F_-(A + F_-)} - \dfrac{1}{F_-} \right] & \text{for } y \in (0,\, L/2) \\ \dfrac{\langle \dot{y} \rangle}{L} \left[\dfrac{(1 - e^{-\phi_2})(A - F_+)}{kF_+} \delta_+(y - L/2) \right. & \\ \left. \quad + \dfrac{A\, e^{2\phi_2 (y/L - 1)}}{F_+(A + F_+)} - \dfrac{1}{F_+} \right] & \text{for } y \in (L/2,\, L) \end{cases}, \tag{14}$$

where $\delta_\pm(x)$ are the half Dirac-δ functions [21].

Correspondingly, the drift velocity for $A > F_+$ or $0 < A < F_-$ is given by

$$\langle \dot{x} \rangle = v_0 \, \frac{1 - e^{\phi_1 + \phi_2} - \dfrac{2A^2 v}{LkF_+F_-}(1 - e^{\phi_1})(1 - e^{\phi_2})}{1 - e^{\phi_1 + \phi_2} - \dfrac{2A^2 v_0}{LkF_+F_-}(1 - e^{\phi_1})(1 - e^{\phi_2})}, \tag{15}$$

and for $F_- < A < F_+$ by

$$\langle \dot{x} \rangle = v - \left[\frac{1}{v - v_0} - \frac{(1 - e^{\phi_1})(F_- - A)^2}{2kLF_-^2} + \frac{(1 - e^{-\phi_2})(F_+ - A)^2}{2kLF_+^2} \right]^{-1}, \qquad (16)$$

where, recall, $v_0 = b^2 v$ is the deterministic value of the Stokes' drift velocity for the square wave. We mention some limiting cases of interest. (i) The limit $A \to 0$ or $k \to \infty$ leads to the deterministic Stokes' velocity, $\langle \dot{x} \rangle = v_0$. (ii) The drift velocity derived in Ref. [16] is recovered in the white noise limit $A \to \infty$, $k \to \infty$, with a finite $D = A^2/2k$. (iii) The quenched-noise limit $k \to 0$ describes the system in which half of the particles, chosen at random, are subjected to a constant external forcing $+A$ and the other half to forcing $-A$. When there are no fixed points, the mean velocity in this limit is

$$\langle \dot{x} \rangle = v_0 \left(\frac{v^2}{v^2 - A^2} \right). \qquad (17)$$

This expression clearly indicates the existence of the flux reversal suggested earlier, since the drift velocity is negative for sufficiently large amplitude A of the forcing, and positive for small A's. When there are fixed points in the "+" dynamics, Eq. (16) leads to a mean velocity

$$\langle \dot{x} \rangle = \frac{F_+^2 + F_-^2 - 2A^2}{4(v + A)}. \qquad (18)$$

In this limit, the current is reversed at $A = \sqrt{(F_+^2 + F_-^2)/2} = \sqrt{1 + b^2}\, v$.

Figure 1 shows the drift velocity, Eqs. (15) and (16), as a function of the normalized transition rate, $\beta = 2kvL/A^2$. The plots of the analytic results are in good agreement with the Monte Carlo simulation of the original stochastic differential equation (2). When the transition rate is high ($\beta \gg 1$), the effect of the dichotomous noise is averaged out and the drift velocity approaches the deterministic limit v_0 regardless of the noise amplitude. Interesting phenomena, namely, negative drift velocity and current reversal, take place only when the transition rate is sufficiently small, i.e., $\beta \lesssim 1$.

Figure 2 shows the drift velocity, Eqs. (15) and (16), in the three different regimes corresponding to low ($A < F_-$) and high ($A > F_+$) noise amplitudes with no fixed point, and intermediate ($F_- < A < F_+$) noise amplitudes with a pair of fixed points. The agreement between analytic results and simulation is again very good. At low noise amplitudes the drift velocity is positive and increases with increasing noise amplitude, i.e., noise enhances Stokes' drift. The noise-induced enhancement reaches its maximum at $A = F_-$ and decreases above this noise amplitude. In general, noise-induced phenomena disappear when the noise becomes too large. However, the decrease at the intermediate noise is not the destruction of the Stokes' drift due to large fluctuations of the particle velocity. The sudden change with discontinuity in the first derivative of the drift velocity suggests the appearance of a bifurcation in the dynamics. When $F_- < A < F_+$, the system has a stable fixed point in the "+" dynamics and some particles become stuck at the fixed point until

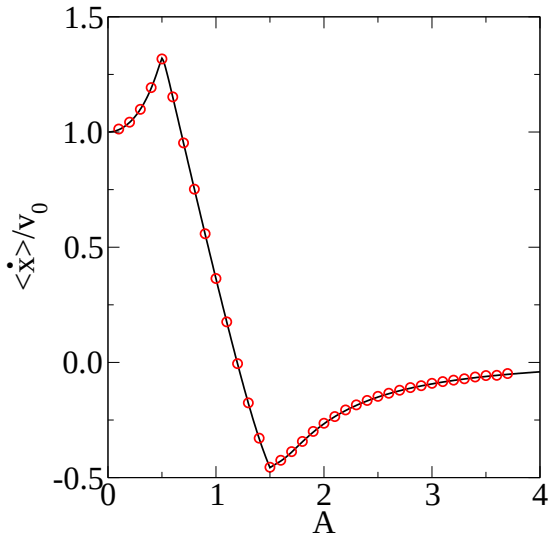

Fig 2. The asymptotic Stokes' drift velocity (normalized by its deterministic value $v_0 = b^2 v$) as a function of the noise amplitude A. The solid line represents theory and the circles show the results of numerical simulations. The values of the parameters are $v = 1$, $b = 0.5$, $k = 1$, and $L = 1$.

the noise switches. The actual drift takes place only when the system is in the "–" dynamics, corresponding to a smaller or even negative value of $\dot{x}$. The negative drift reaches its maximum at $A = F_+$ where the fixed points disappear. For $A > F_+$, the "±" dynamics correspond to drift velocities in opposite directions, and therefore the net drift is reduced. Finally, as expected, Stokes' drift is asymptotically destroyed as the noise amplitude increases to infinity.

Figure 3 illustrates the probability densities Eqs. (12), (14) for three different amplitudes of the dichotomous noise. For comparison, the numerical solution of the stochastic differential equation (2) is also shown. The agreement between the present analytic theory and the computer simulation is nearly perfect. Due to the discontinuity of the square wave $F(y)$, Eq. (10), the probability densities are discontinuous at $y = 0$ and $y = L/2$ for all cases. Moreover, for $A = 1.0$ the system has fixed points and the probability density becomes δ-singular at the stable fixed point. The probability densities are also asymmetric in all cases. For $A = 0.4$, the density is higher at $y \in (0, L/2)$ than at $y \in (L/2, L)$. On the other hand, the situation is the other way around for $A = 1.6$. This difference causes the current reversal.

3. Hypersensitive Transport

Generally and somewhat loosely speaking, the term "hypersensitive transport" refers to a highly nonlinear directed response of a nonequilibrium, noisy system to a small systematic external forcing. This phenomenon was discovered rather recently, and received a great deal of theoretical [9, 12] and experimental [13] attention.

One of the simplest models exhibiting this novel phenomenon describes an over-

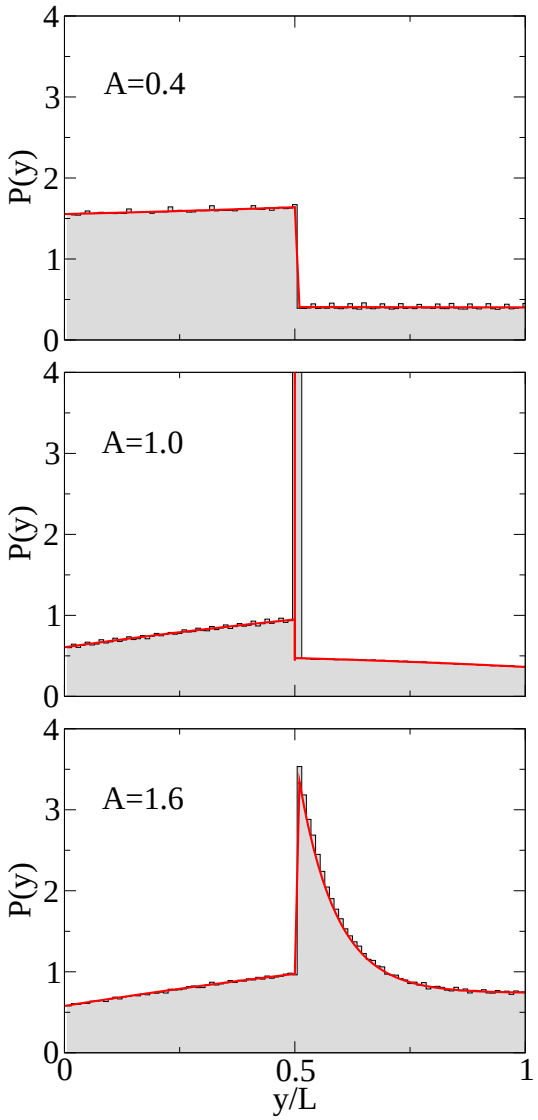

Fig 3. The profile of the probability density $P(y)$ for three values of the amplitude A of the dichotomous noise. The first ($A < F_-$) and the last panel ($A > F_+$) correspond to the regime with no fixed points, while the second panel ($F_- < A < F_+$) corresponds to the presence of two fixed points. Solid lines indicate the analytic results and shaded histograms show the results of numerical simulation. The values of the parameters are $v = 1$, $b = 0.5$, $k = 1$, and $L = 1$. In the simulation, the dynamics of 20000 particles is sampled at 100 different times.

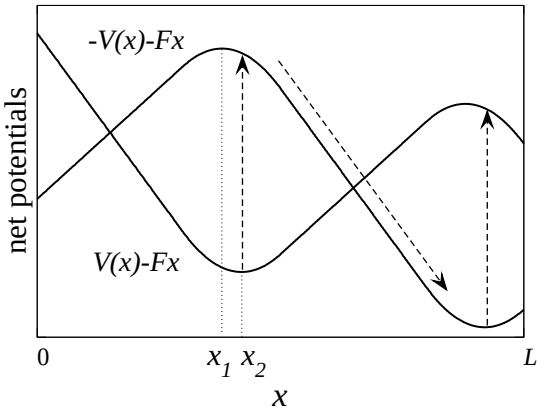

Fig 4. The net potentials $\mp V(x) - Fx$. x_1 and x_2 represent unstable and stable fixed points, respectively. The substrate potential is defined as $V(x) = -\int^x v(x')dx'$. When the switching rate between these two potentials is sufficiently small, particles accumulate at a stable fixed point x_2, bypassing the unstable fixed point x_1. When the potential switches, the particles are repelled by the unstable fixed point x_1 toward a new stable fixed point. Even when the external force F is very small, the particles are able to avoid backward drift.

damped particle whose dynamics switches dichotomically between a symmetric potential and its negative. When the symmetry of the system is slightly broken by a small directed external force, the system responds highly nonlinearly by exhibiting a "giant" systematic particle drift. Let us thus consider the following stochastic dynamics with a multiplicative noise [9]:

$$\dot{x} = F + \xi(t)v(x). \tag{19}$$

The dichotomous noise $\xi(t) = \pm 1$ has, as before, transition rate k. $F > 0$ represents a constant external force, and $v(x)$ is a given symmetric "substrate" force profile that is assumed to be periodic, $v(x + L) = v(x)$. Some preliminary results on this model were reported in Ref. [9]. Here we present more (and more detailed) results than in our earlier work.

3.1. *No fixed points*

When the external force is sufficiently large [$F^2 - v^2(x) \neq 0$ for any $x \in [0, L)$], there is no fixed point in either dynamics, and one obtains the asymptotic probability density

$$P(x) = \frac{\langle \dot{x} \rangle}{LF} \left\{ 1 + \frac{v(x) \displaystyle\int_x^{x+L} dz\, v'(z) \exp\left[-\int_z^x dw \frac{2kF}{F^2 - v^2(w)} \right]}{[F^2 - v^2(x)] \left\{ \exp\left[\displaystyle\int_0^L dz \frac{2kF}{F^2 - v^2(z)} \right] - 1 \right\}} \right\}, \tag{20}$$

and, through the normalization of $P(x)$, the mean asymptotic velocity

$$\frac{\langle \dot{x} \rangle}{F} = \left\{ 1 + \frac{\displaystyle\int_0^L dx \, \frac{v(x)}{F^2 - v^2(x)} \int_x^{x+L} dz \; v'(z) \exp\left[- \int_z^x dw \frac{2kF}{F^2 - v^2(w)} \right]}{\displaystyle L \left\{ \exp\left[\int_0^L dz \frac{2kF}{F^2 - v^2(z)} \right] - 1 \right\}} \right\}^{-1} . \tag{21}$$

3.2. *Asymptotic dynamics with fixed points*

For simplicity and without the loss of any relevant point of the method, we take $v(x)$ to be a continuously decreasing function in $[0, L/2]$ and symmetric about $L/2$, $v(x + L/2) = -v(x)$. This implies that $P(x + L/2) = P(x)$, so that we can limit our analysis to half a period. When the external force is weak, the particle moves alternately in the two "net potentials" represented schematically in Fig. 4. In this simple case the equation $F^2 - v^2(x) = 0$ has only two solutions in $[0, L/2]$, x_1, corresponding to an unstable fixed point in the "$-$" dynamics [$F = v(x_1)$, $v'(x_1) < 0$], and x_2, a stable fixed point in the "+" dynamics [$F = -v(x_2)$, $v'(x_2) < 0$], with $x_2 > x_1$. These fixed points are the local extrema of the net potentials.

According to the discussions in [9,10], the physically acceptable solution in the interval $[x_2 - L/2, x_2]$ is given by

$$\begin{aligned} P(x) = & \frac{\langle \dot{x} \rangle}{LF} \left\{ 1 + \frac{v(x)}{|F^2 - v^2(x)|} \int_{x_1}^x dz \, \mathrm{sgn}\left[F^2 - v^2(z) \right] v'(z) \right. \\ & \left. \times \exp\left[- \int_z^x dw \frac{2kF}{F^2 - v^2(w)} \right] \right\}, \end{aligned} \tag{22}$$

which extends by periodicity to the whole x-axis. At the unstable fixed point x_1, the probability density is continuous and its value is given by

$$\lim_{x \searrow x_1} P(x) = \lim_{x \nearrow x_1} P(x) = \frac{\langle \dot{x} \rangle}{LF \left\{ 1 - 1/[2(k/|v'(x_1)| + 1)] \right\}}. \tag{23}$$

Note that the stable fixed points $x_2 - L/2$ and x_2 are located at the ends of the chosen interval and there is no other stable fixed point within this interval. Therefore, the probability density is continuous inside the interval. However, it can be singular at the stable fixed points. When the transition rate is sufficiently large [$k/|v'(x_2)| > 1$], there is not enough time for the particles to reach and to accumulate at the stable fixed points, and thus $P(x)$ is continuous x_2 and $x_2 - L/2$ as follows:

$$\lim_{x \nearrow x_2} P(x) = \lim_{x \searrow (x_2 - L/2)} P(x) = \frac{\langle \dot{x} \rangle}{LF \left\{ 1 + 1/[2(k/|v'(x_2)| - 1)] \right\}}. \tag{24}$$

For low transition rates [$k/|v'(x_2)| \leqslant 1$], the majority of particles become stuck near the stable fixed points for a long time, thus resulting in the divergence of $P(x)$ at x_2 and $x_2 - L/2$. These divergences cause a highly nonlinear conductivity of the system, as discussed later.

From the normalization of $P(x)$, the average velocity is obtained as

$$\frac{\langle \dot{x} \rangle}{F} = \left\{ 1 + \frac{2}{L} \int_{x_2 - L/2}^{x_2} dx \, \frac{v(x)}{|F^2 - v^2(x)|} \right. \\ \left. \times \int_{x_1}^{x} dz \, \mathrm{sgn}\left[F^2 - v^2(z)\right] v'(z) \exp\left[- \int_z^x dw \frac{2kF}{F^2 - v^2(w)} \right] \right\}^{-1}. \tag{25}$$

Although exact, the above results are still too complicated to gain a clear physical picture of the behavior of the system. We therefore turn to a particular shape of the velocity profile $v(x)$ that simplifies the evaluation of the above functional expressions.

3.3. *Piecewise linear internal force*

We consider a piecewise linear "substrate" force

$$v(x) = \begin{cases} v_0, & \text{for } x \in [0, L/2 - 2l) \\ v_0 \left[L/(2l) - 1 - x/l \right], & \text{for } x \in [L/2 - 2l, L/2) \\ -v(x - L/2) & \text{for } x \in [L/2, L) \end{cases} \tag{26}$$

with $l \leqslant L/4$ and the periodicity condition $v(x + L) = v(x)$. It is convenient to introduce the following dimensionless variables:

$$f = F/v_0, \qquad \alpha = lk/v_0, \qquad \Gamma = 4l/L \quad (0 < \Gamma < 1), \tag{27}$$

and to work with the function

$$T(x) = \frac{1}{v_0} \int_0^x dz \, \mathrm{sgn}\left[F^2 - v^2(z)\right] v'(z) \exp\left[\int_0^z dw \frac{2kF}{F^2 - v^2(w)} \right]$$

$$= \begin{cases} 0 & \text{for } x \in [0, L/2 - 2l) \\ \left| \dfrac{f+1}{f-1} \right|^{\alpha} \exp\left[- \dfrac{4\alpha f (1 - \Gamma)}{(1 - f^2)\Gamma} \right] & \\ \times \displaystyle\int_1^{\chi} ds \, \mathrm{sgn}(f^2 - s^2) \left| \frac{f - s}{f + s} \right|^{\alpha} & \text{for } x \in [L/2 - 2l, L/2) \end{cases}, \tag{28}$$

where $\chi = L/(2l) - 1 - x/l$.

In the absence of fixed points ($f > 1$), one obtains the stationary probability

density

$$P(x)=\begin{cases}\dfrac{\langle\dot{x}\rangle}{LF}\left\{1-\dfrac{T(L/2)}{(f^2-1)(\Delta+1)}\right. & \\ \qquad\left.\times\exp\left[-\dfrac{8\alpha f}{(f^2-1)\Gamma}\dfrac{x}{L}\right]\right\} & \text{for } x\in[0,L/2-2l) \\ \dfrac{\langle\dot{x}\rangle}{LF}\left\{1+\left(\dfrac{f+1}{f-1}\right)^{\alpha}\right. & \\ \qquad\left.\times\dfrac{\chi\left[T(x)-T(L/2)/(\Delta+1)\right]}{\Delta(f-\chi)^{1+\alpha}(f+\chi)^{1-\alpha}}\right\} & \text{for } x\in[L/2-2l,L/2)\end{cases}, \tag{29}$$

where we have introduced the short-hand notation

$$\Delta=\left|\frac{f+1}{f-1}\right|^{2\alpha}\exp\left[\frac{4\alpha f(1-\Gamma)}{(f^2-1)\Gamma}\right]. \tag{30}$$

The corresponding mean velocity is given by

$$\begin{aligned}\frac{\langle\dot{x}\rangle}{F}=&\left\{1-\frac{\Gamma T(L/2)}{4\alpha f(\Delta+1)}\left[1-\Delta^{-1}\left(\frac{f+1}{f-1}\right)^{2\alpha}\right]+\frac{\Gamma}{2\Delta}\left(\frac{f+1}{f-1}\right)^{\alpha}\right. \\ &\left.\times\int_{-1}^{1}dt\,\frac{t\left[T(L/2-l(t+1))-T(L/2)/(\Delta+1)\right]}{(f-t)^{1+\alpha}(f+t)^{1-\alpha}}\right\}^{-1}.\end{aligned} \tag{31}$$

When $0<f<1$ the dynamics has two fixed points, an unstable one at $x_1=L/2-l(1+f)$ and a stable one at $x_2=L/2-l(1-f)$. The situation is then more complicated but still analytically tractable. The probability density is written separately for three different regions:

$$P(x)=\begin{cases}\dfrac{\langle\dot{x}\rangle}{LF}\left\{1-\dfrac{T(x_1)}{1-f^2}\exp\left[\dfrac{8\alpha f}{(1-f^2)\Gamma}\dfrac{x}{L}\right]\right\} & \text{for } x\in[0,L/2-2l) \\ \dfrac{\langle\dot{x}\rangle}{LF}\left\{1+\left(\dfrac{1+f}{1-f}\right)^{\alpha}\right. & \\ \qquad\left.\times\dfrac{\chi\left[T(x)-T(x_1)\right]}{\Delta\left|f-\chi\right|^{1+\alpha}\left|f+\chi\right|^{1-\alpha}}\right\} & \text{for } x\in[L/2-2l,x_2) \\ \dfrac{\langle\dot{x}\rangle}{LF}\left\{1+\left(\dfrac{1+f}{1-f}\right)^{\alpha}\right. & \\ \qquad\left.\times\dfrac{\chi\left[T(x)+\Delta T(x_1)-T(L/2)\right]}{\Delta\left|f-\chi\right|^{1+\alpha}\left|f+\chi\right|^{1-\alpha}}\right\} & \text{for } x\in[x_2,L/2)\end{cases}. \tag{32}$$

This probability density is continuous at the unstable fixed point x_1,

$$\lim_{x\searrow x_1}P(x)=\lim_{x\nearrow x_1}P(x)=\frac{\langle\dot{x}\rangle}{LF\left\{1-1/[2(\alpha+1)]\right\}}. \tag{33}$$

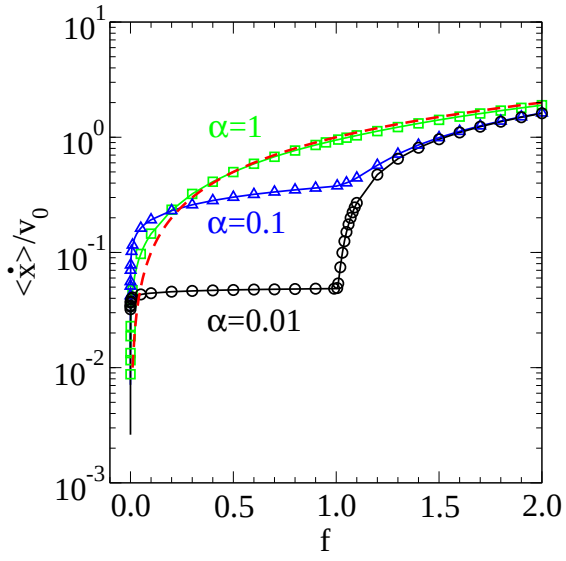

Fig 5. The mean asymptotic velocity as a function of the applied force f for different values of the parameter α. The other parameters are $v_0 = 1$, $\Gamma = 0.4$, and $L = 1$. The symbols represent the results of numerical simulations. The solid lines are the result of theory and the dashed line indicates the linear response.

At the stable fixed point x_2, $P(x)$ is continuous for $\alpha > 1$, with

$$\lim_{x \searrow x_2} P(x) = \lim_{x \nearrow x_2} P(x) = \frac{\langle \dot{x} \rangle}{LF\left\{1 + 1/[2(\alpha - 1)]\right\}}, \tag{34}$$

but divergent and integrable for $\alpha \leqslant 1$. The average velocity as usual follows from the normalization of $P(x)$,

$$\begin{aligned} \frac{\langle \dot{x} \rangle}{F} = & \left\{ 1 - \frac{\Gamma T(x_1)}{4\alpha f} \left[\left(\frac{1+f}{1-f} \right)^{2\alpha} \Delta^{-1} - 1 \right] + \frac{\Gamma (1+f)^{\alpha}}{2\Delta (1-f)^{\alpha}} \right. \\ & \times \left\{ \int_{-1}^{1} dt \, \frac{t\big[T[L/2 - l(t+1)] - T(x_1)\big]}{|t-f|^{1+\alpha} \, |t+f|^{1-\alpha}} + [T(x_1)(1+\Delta) - T(L/2)] \right. \\ & \left. \left. \times \int_{-1}^{-f} dt \, \frac{t}{|t-f|^{1+\alpha} \, |t+f|^{1-\alpha}} \right\} \right\}^{-1}. \end{aligned} \tag{35}$$

The integrals in Eqs. (28), (31), and (35) cannot be evaluated in closed analytic form except for a few specific values of α. As an illustration, in Appendix B we present closed analytic results for $\alpha = 1/2$.

3.4. *Response Properties*

Equations (31) and (35) are numerically evaluated and plotted in Fig. 5 as a function of the external force f for different values of α. The results are in good agreement

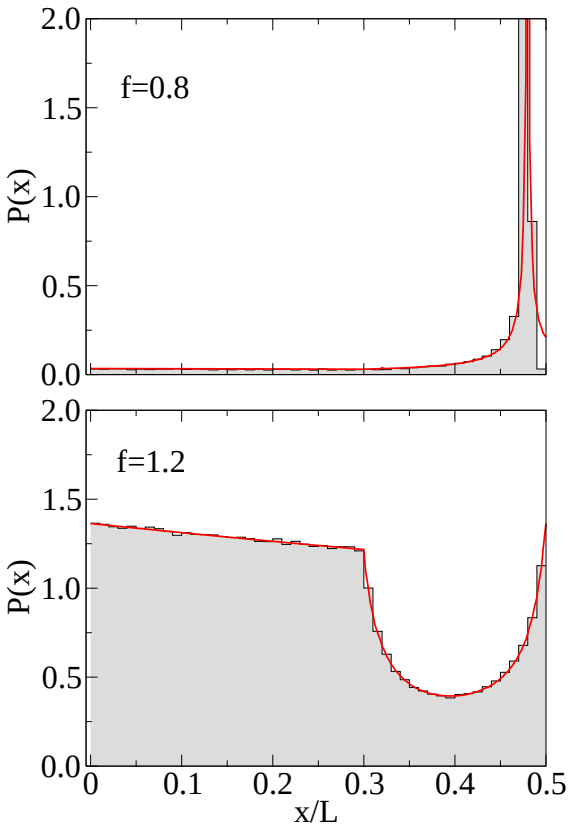

Fig 6. The profile of the probability density $P(x)$ for two values of the applied force f. The first corresponds to the regime with fixed points, and the second to the regime with no fixed points. Solid lines indicate the analytic results and shaded histograms show the results of numerical simulations. The values of the other parameters are $v_0 = 1$, $\alpha = 1$, $\Gamma = 0.4$, and $L = 1$. In the simulations, the dynamics of 20000 particles is sampled at 100 different times.

with computer simulations. The drift velocity shows highly nonlinear responses to the external force depending on the transition rate of the dichotomous noise, as illustrated in Fig. 5. There are four asymptotic regimes of interest.

(i) *Linear Response Regime I*: When the deterministic external force f is much larger than the fluctuating force ($f \gg 1$), the effect of the fluctuating force is negligible and a linear response, $\langle \dot{x} \rangle / v_0 = f$, is expected for any transition rate. Indeed, all curves in Fig. 5 approach the linear response curve as f increases.

(ii) *Linear Response Regime II*: When the transition rate is very high ($\alpha \gg 1$), the fluctuating force is averaged out and only the deterministic external force effectively drives the particles. Therefore, a linear response, $\langle \dot{x} \rangle / v_0 = f$, is again expected for $\alpha \gg 1$. Figure 5 shows that the drift velocity for $\alpha = 1$ is already very close to this linear response limit.

(iii) *Adiabatic Regime:* Since we are interested in nonlinear response, we focus

on the cases with small α and small f. When the transition rate is sufficiently small (adiabatic limit), the system remains in one of the $\pm V(x)$ potentials for a long time. The particles eventually reach a minimum of the net potential and wait there until the potential flips. When the dichotomous noise switches its value, the particles suddenly find themselves near the maximum of the net potential as illustrated in Fig. 4. They move down to a new potential minimum and wait again for the next potential flip. A typical time for them to escape from the region close to the maximum is given by $\tau = -(\ell/v_0)\ln f$. Therefore, this adiabatic regime is realized when the average time between switches, k^{-1}, is much longer than τ, which leads to $1 > f \gg \exp(-1/\alpha)$. (Note that the adiabatic regime is not possible unless there is a fixed point and thus $f < 1$.) Only $\alpha \ll 1$ can satisfy this condition. In this range of the external force, the mean velocity is simply half the spatial period of the "substrate" potential divided by the mean switching time, that is, $\langle \dot{x} \rangle = Lk/2 = 2v_0\alpha/\Gamma$. The same result can be obtained directly from Eq. (35) by taking the appropriate limit. This result is interesting in that the mean velocity does not depend on the external force F, nor the magnitude v_0 of the fluctuating force, and is inversely proportional to the correlation time of the noise. A higher transition rate reduces the waiting period at the potential minimum and thus increases the mean velocity. However, increasing k reduces the range of occurrence of this adiabatic regime. These results are in perfect agreement with the computer simulations (Fig. 5). The transport in the adiabatic regime has been investigated as hypersensitive response in Ref. [12] but without a full analytic solution.

(iv) *Hyper-Nonlinear Regime:* For a small external force, $f < \exp(-1/\alpha)$, the particles manage to advance to the next potential minimum only when the dichotomous noise realizes exponentially rare cases where it keeps the same value for times much longer than the correlation time. Therefore, the mean velocity rapidly falls to zero as f decreases. Indeed, from Eq. (35), taking the limit $f \to 0$, we find for the mean velocity

$$\langle \dot{x} \rangle / v_0 \approx [2\alpha\Gamma(\ln f)^2]^{-1}. \tag{36}$$

This result is striking in that the susceptibility (or the conductance) of the system $d\langle \dot{x} \rangle / df$ diverges at $f = 0$, indicating that the mean velocity is extremely sensitive to the external force. Another interesting feature is that the mean velocity is inversely proportional to the transition rate k, in contrast to the adiabatic regime where the velocity is directly proportional to the transition rate. Figure 5 shows the mean velocity as a function of the applied force f for different values of α. Note the linear response regime I for all values of α; the linear response regime II for $\alpha = 1$ (practically for all f, except the small-f region); the adiabatic regime for $\alpha = 0.01$ and (more restricted) for $\alpha = 0.1$; and the hyper-nonlinear regime for all α. The nonmonotonic dependence of the mean velocity on α (e.g., $\sim \alpha$ in the adiabatic regime, $\sim \alpha^{-1}$ in the hyper-nonlinear regime, and α-independent in the linear response regime) leads to the fact that the curves in Fig. 5 cross each other in the f-regions where there is a switch between these various regimes.

In Fig. 6 we present two typical profiles of the probability density $P(x)$ for the two regimes with and without fixed points, with an abrupt change in shape between these regimes.

4. Conclusions

We have derived explicit results for the probability density and drift velocity in systems that model Stokes' drift and hypersensitive response driven by dichotomous noise. We include the situation in which the asymptotic dynamics crosses unstable fixed points, a case where the standard approaches are not applicable in a straightforward way [9, 10]. We have presented analytic results for particular choices of potentials and parameters that elucidate the behavior in a way not entirely possible when only numerical results are available.

Appendix A. Stokes' Drift Problem: Results for the Piecewise Linear Wave Eq. (10)

In the absence of fixed points one finds the following general piecewise expression for the probability density in four different regions:

$$P(y) = \begin{cases} \dfrac{\langle \dot{y} \rangle}{L} \left[C_1 \, e^{2\phi_1 y/L} - \dfrac{1}{F_-} \right] & \text{for } y \in [0, L/2 - 2l) \\ \dfrac{\langle \dot{y} \rangle}{L} \dfrac{\mathrm{sgn}[F^2(y) - A^2]}{\left| F^2(y) - A^2 \right|^{1-\alpha}} & \\ \quad \times \left[\dfrac{(2\alpha - 1)k}{\alpha} \displaystyle\int_{L/2-2l}^{y} \dfrac{dz}{\left| F^2(z) - A^2 \right|^{\alpha}} + C_2 \right] & \text{for } y \in [L/2 - 2l, L/2) \\ \dfrac{\langle \dot{y} \rangle}{L} \left[C_3 \, e^{\phi_2 (2y/L - 1)} - \dfrac{1}{F_+} \right] & \text{for } y \in [L/2, L - 2l) \\ \dfrac{\langle \dot{y} \rangle}{L} \dfrac{\mathrm{sgn}[F^2(y) - A^2]}{\left| F^2(y) - A^2 \right|^{1+\alpha}} & \\ \quad \times \left[\dfrac{(2\alpha + 1)k}{\alpha} \displaystyle\int_{L-2l}^{y} dz \, \left| F^2(z) - A^2 \right|^{\alpha} + C_4 \right] & \text{for } y \in [L - 2l, L) \end{cases} \tag{A.1}$$

where we have used the dimensionless quantities $\alpha = lk/bv$, and ϕ_1, ϕ_2 as defined in Eq. (13). Note that the system is invariant under the transformation, $y \to (y - L/2)$ and $b \to -b$. Therefore, $P(y)$ for $y > L/2$ can formally be obtained from the expression for $P(y - L/2)$ by simply changing b to $-b$ and (*nota bene*) α to $-\alpha$. The integration constants C_1–C_4 assure that $P(y)$ has no discontinuity in this case and is periodic. The mean asymptotic velocity $\langle \dot{x} \rangle = v + \langle \dot{y} \rangle$ is obtained by imposing the normalization of $P(y)$.

We turn now to the case of principal interest to us, $F_- < A < F_+$, where the dynamics exhibits two fixed points, one stable, $y_1 = L/2 - 2l + l\,[A - F_-]\,/(bv)$, and one unstable, $y_2 = L - 2l + l\,[F_+ - A]\,/(bv)$. The piecewise expression for the

probability density is now given by

$$P(y) = \begin{cases} \dfrac{\langle \dot{y} \rangle}{L} \left[D_1 e^{2\phi_1 y/L} - \dfrac{1}{F_-} \right] & \text{for } y \in [0, L/2 - 2l) \\ \dfrac{\langle \dot{y} \rangle}{L} \dfrac{1}{\left[A^2 - F^2(y)\right]^{1-\alpha}} \left\{ D_2 - \dfrac{k(2\alpha-1)}{\alpha} \right. & \\ \qquad \left. \times \displaystyle\int_{L/2-2l}^{y} dz \ \left[F^2(z) - A^2\right]^{-\alpha} \right\} & \text{for } y \in [L/2 - 2l, y_1) \\ \dfrac{\langle \dot{y} \rangle}{L} \dfrac{1}{\left[F^2(y) - A^2\right]^{1-\alpha}} \left\{ D_3 - \dfrac{k(2\alpha-1)}{\alpha} \right. & \\ \qquad \left. \times \displaystyle\int_{y}^{L/2} dz \ \left[A^2 - F^2(z)\right]^{-\alpha} \right\} & \text{for } y \in [y_1, L/2) \\ \dfrac{\langle \dot{y} \rangle}{L} \left\{ D_4 \, e^{2\phi_2 (y/L - 1/2)} - \dfrac{1}{F_+} \right\} & \text{for } y \in [L/2, L - 2l) \\ \dfrac{\langle \dot{y} \rangle}{L} \dfrac{k(2\alpha+1)}{\alpha \ \left|F^2(y) - A^2\right|^{1+\alpha}} & \\ \qquad \times \displaystyle\int_{y_2}^{y} dz \ \mathrm{sgn}\left[F^2(z) - A^2\right] \left|F^2(z) - A^2\right|^{\alpha} & \text{for } y \in [L - 2l, L) \end{cases} \tag{A.2}$$

The integration constants D_1–D_4 are obtained by imposing the continuity of $P(y)$ at $y = L/2 - 2l$, $L/2$, and $L - 2l$, and its periodicity. Note from Eq. (A.2) that $P(y)$ is continuous at y_2, $\lim_{y \nearrow y_2} P(y) = \lim_{y \searrow y_2} P(y) = -(\langle \dot{y} \rangle / L)[(2\alpha+1)]/[2(\alpha+1)A]$. Also, $\langle \dot{y} \rangle < 0$ [from the positiveness of $P(y_2)$]. At the stable fixed point, $P(y)$ is either divergent, with a weak, integrable singularity whenever $\alpha \leqslant 1$, or finite, $\lim_{y \nearrow y_1} P(y) = \lim_{y \searrow y_1} P(y) = -(\langle \dot{y} \rangle / L)[(2\alpha-1)][2(\alpha-1)A]$ when $\alpha > 1$. Finally, the mean velocity is obtained by imposing the normalization condition for $P(y)$.

The integrals that appear in the expressions (A.1) and (A.2) of $P(y)$ and, correspondingly, the integration constants C_1–C_4 and D_1–D_4 can be evaluated in a closed analytic form only for certain values of α. As an example, we present below these results for the particular case $\alpha = 1/2$.

When $A > F_+$, the probability density reads

$$P(y) = \begin{cases} \dfrac{\langle \dot{y} \rangle}{L} \left[C_1 \, e^{2\phi_1 y/L} - \dfrac{1}{F_-} \right] & \text{for } y \in [0, L/2 - 2l) \\ -\dfrac{\langle \dot{y} \rangle}{L} \dfrac{C_2}{[A^2 - F^2(y)]^{1/2}} & \text{for } y \in [L/2 - 2l, L/2) \\ \dfrac{\langle \dot{y} \rangle}{L} \left[C_3 \, e^{\phi_2(2y/L - 1)} - \dfrac{1}{F_+} \right] & \text{for } y \in [L/2, L - 2l) \\ -\dfrac{\langle \dot{y} \rangle}{L} \left\{ \dfrac{F(y)}{[A^2 - F^2(y)]} + \dfrac{A^2 \arcsin[F(y)/A] + C_4}{[A^2 - F^2(y)]^{3/2}} \right\} & \text{for } y \in [L - 2l, L) \end{cases} \tag{A.3}$$

and the corresponding asymptotic velocity

$$\begin{aligned} \langle \dot{x} \rangle = & v + \left\{ C_1 \frac{e^{\phi_1(1-\Gamma)} - 1}{2\phi_1} + C_3 \frac{e^{\phi_2(1-\Gamma)} - 1}{2\phi_2} - \frac{v(1-\Gamma)}{F_+ F_-} \right. \\ & + \frac{\Gamma}{4bv} \left[\left(C_2 - \frac{F_-}{\sqrt{A^2 - F_-^2}} \right) \arcsin\left(\frac{F_-}{A} \right) \right. \\ & - \left(C_2 - \frac{F_+}{\sqrt{A^2 - F_+^2}} \right) \arcsin\left(\frac{F_+}{A} \right) \\ & \left. \left. + \, + \frac{C_4}{A^2} \left(\frac{F_-}{\sqrt{A^2 - F_-^2}} - \frac{F_+}{\sqrt{A^2 - F_+^2}} \right) \right] \right\}^{-1}, \end{aligned} \tag{A.4}$$

where $\Gamma = \dfrac{4l}{L}$ $(0 < \Gamma < 1)$, and $\phi_{1,2} = \dfrac{2bF_{\mp}^2}{\Gamma(F_{\mp}^2 - A^2)}$. The integration constants C_1–C_4 are given by

$$\begin{aligned} C_1 = & \left\{ \frac{A^2 - F_-^2}{A^2 - F_+^2} - e^{(\phi_1 + \phi_2)(1-\Gamma)} \right\}^{-1} \left\{ \frac{A^2 - F_-^2}{F_-(A^2 - F_+^2)} - \frac{\sqrt{A^2 - F_+^2}}{F_+ \sqrt{A^2 - F_-^2}} \right. \\ & - \frac{F_+ \sqrt{A^2 - F_+^2} - F_- \sqrt{A^2 - F_-^2} - A^2[\arcsin(F_+/A) - \arcsin(F_-/A)]}{(A^2 - F_+^2)\sqrt{A^2 - F_-^2}} \\ & \left. + \, e^{\phi_2(1-\Gamma)} \left[\frac{\sqrt{A^2 - F_+^2}}{F_+ \sqrt{A^2 - F_-^2}} - \frac{1}{F_-} \right] \right\}, \end{aligned}$$

$$
\begin{aligned}
C_2 =& \left\{ \frac{A^2-F_-^2}{A^2-F_+^2} - e^{(\phi_1+\phi_2)(1-\Gamma)} \right\}^{-1} \left\{ \frac{(A^2-F_-^2)^{3/2}}{(A^2-F_+^2)F_-} + e^{\phi_1(1-\Gamma)} \right. \\
& \times \left\{ \frac{\sqrt{A^2-F_+^2}}{F_+} - \frac{(A^2-F_-^2)^{3/2}}{(A^2-F_+^2)F_-} - \frac{\sqrt{A^2-F_+^2}e^{\phi_2(1-\Gamma)}}{F_+} \right. \\
& \left. \left. + \frac{F_+\sqrt{A^2-F_+^2} - F_-\sqrt{A^2-F_-^2} + A^2[\arcsin(F_+/A) - \arcsin(F_-/A)]}{A^2-F_+^2} \right\} \right\}, \\
C_3 =& \left\{ \frac{A^2-F_-^2}{A^2-F_+^2} - e^{(\phi_1+\phi_2)(1-\Gamma)} \right\}^{-1} \left\{ \frac{A^2-F_-^2}{F_+(A^2-F_+^2)} - \frac{(A^2-F_-^2)^{3/2}}{F_-(A^2-F_+^2)^{3/2}} \right. \\
& - \left[\frac{F_+\sqrt{A^2-F_+^2} - F_-\sqrt{A^2-F_-^2} + A^2[\arcsin(F_+/A) - \arcsin(F_-/A)]}{(A^2-F_+^2)^{3/2}} \right. \\
& \left. \left. - \frac{(A^2-F_-^2)^{3/2}}{F_-(A^2-F_+^2)^{3/2}} + \frac{1}{F_+} \right] e^{\phi_1(1-\Gamma)} \right\}, \\
C_4 =& \left\{ \frac{A^2-F_-^2}{A^2-F_+^2} - e^{(\phi_1+\phi_2)(1-\Gamma)} \right\}^{-1} \left\{ \frac{\sqrt{A^2-F_+^2}(A^2-F_-^2)}{F_+} \right. \\
& + \frac{(A^2-F_-^2)F_+\sqrt{A^2-F_+^2} + A^2\arcsin(F_+/A)]}{A^2-F_+^2} \\
& + e^{\phi_2(1-\Gamma)} \left[\frac{(A^2-F_-^2)^{3/2}}{F_-} - \frac{\sqrt{A^2-F_+^2}(A^2-F_-^2)}{F_+} \right] \\
& \left. - e^{(\phi_1+\phi_2)(1-\Gamma)} \left[F_-\sqrt{A^2-F_-^2} + A^2\arcsin(F_-/A) + \frac{(A^2-F_-^2)^{3/2}}{F_-} \right] \right\}.
\end{aligned}
\tag{A.5}
$$

For $0 < A < F_-$, one obtains the probability density

$$P(y) = \begin{cases} \dfrac{\langle \dot{y} \rangle}{L} \left[C_1' e^{2\phi_1 y/L} - \dfrac{1}{F_-} \right] & \text{for } y \in [0, L/2 - 2l) \\ \dfrac{\langle \dot{y} \rangle}{L} \dfrac{C_2'}{\sqrt{F^2(y) - A^2}} & \text{for } y \in [L/2 - 2l, L/2) \\ \dfrac{\langle \dot{y} \rangle}{L} \left\{ C_3' e^{\phi_2(2y/L - 1)} - \dfrac{1}{F_+} \right\} & \text{for } y \in [L/2, L - 2l) \\ \dfrac{\langle \dot{y} \rangle}{L} \left\{ \dfrac{F(y)}{[F^2(y) - A^2]} \right. & \\ \left. + \dfrac{A^2 \ln \left[\dfrac{\sqrt{F^2(y) - A^2} - F(y)}{A} \right] + C_4'}{[F^2(y) - A^2]^{3/2}} \right\} & \text{for } y \in [L - 2l, L) \end{cases} \tag{A.6}$$

and the corresponding asymptotic drift velocity

$$\begin{aligned} \langle \dot{x} \rangle = & v + \left\{ C_1' \frac{e^{\phi_1(1-\Gamma)} - 1}{2\phi_1} + C_3' \frac{e^{\phi_2(1-\Gamma)} - 1}{2\phi_2} - \frac{v(1-\Gamma)}{F_+ F_-} \right. \\ & + \frac{\Gamma}{4bv} \left[\left(C_2' - \frac{F_+}{\sqrt{F_+^2 - A^2}} \right) \ln \left(\frac{\sqrt{F_+^2 - A^2} + F_+}{A} \right) \right. \\ & - \left(C_2' - \frac{F_-}{\sqrt{F_-^2 - A^2}} \right) \ln \left(\frac{\sqrt{F_-^2 - A^2} + F_-}{A} \right) \\ & \left. \left. + \frac{C_4'}{A^2} \left(\frac{F_-}{\sqrt{F_-^2 - A^2}} - \frac{F_+}{\sqrt{F_+^2 - A^2}} \right) \right] \right\}^{-1} . \end{aligned} \tag{A.7}$$

The integration constants C_1'-C_4' are given by

$$\begin{aligned} C_1' = & \left[\frac{F_-^2 - A^2}{F_+^2 - A^2} - e^{(\phi_1 + \phi_2)(1-\Gamma)} \right]^{-1} \left[e^{\phi_2(1-\Gamma)} \left[\frac{\sqrt{F_+^2 - A^2}}{F_+ \sqrt{F_-^2 - A^2}} - \frac{1}{F_-} \right] \right. \\ & + \frac{F_-^2 - A^2}{F_-(F_+^2 - A^2)} - \frac{\sqrt{F_+^2 - A^2}}{F_+ \sqrt{F_-^2 - A^2}} + \frac{F_+ \sqrt{F_+^2 - A^2} - F_- \sqrt{F_-^2 - A^2}}{(F_+^2 - A^2)\sqrt{F_-^2 - A^2}} \\ & \left. + \frac{A^2}{(F_+^2 - A^2)\sqrt{F_-^2 - A^2}} \ln \left(\frac{\sqrt{F_-^2 - A^2} + F_-}{\sqrt{F_+^2 - A^2} + F_+} \right) \right] , \end{aligned}$$

$$
\begin{aligned}
C_2' = & \left[\frac{F_-^2-A^2}{F_+^2-A^2} - e^{(\phi_1+\phi_2)(1-\Gamma)}\right]^{-1} \left\{ -\frac{(F_-^2-A^2)^{3/2}}{(F_+^2-A^2)F_-} + e^{\phi_1(1-\Gamma)} \right. \\
& \times \left[-\frac{\sqrt{F_+^2-A^2}}{F_+} + \frac{(F_-^2-A^2)^{3/2}}{(F_+^2-A^2)F_-} + \frac{\sqrt{F_+^2-A^2}e^{\phi_2(1-\Gamma)}}{F_+} \right. \\
& \left. \left. + \frac{F_+\sqrt{F_+^2-A^2}-F_-\sqrt{F_-^2-A^2}}{F_+^2-A^2} + \frac{A^2}{F_+^2-A^2}\ln\left(\frac{\sqrt{F_-^2-A^2}+F_-}{\sqrt{F_+^2-A^2}+F_+}\right)\right]\right\}, \\
C_3' = & \left[\frac{F_-^2-A^2}{F_+^2-A^2} - e^{(\phi_1+\phi_2)(1-\Gamma)}\right]^{-1} \left\{ \frac{F_-^2-A^2}{F_+(F_+^2-A^2)} - \frac{(F_-^2-A^2)^{3/2}}{F_-(F_+^2-A^2)^{3/2}} \right. \\
& + \left[\frac{F_+\sqrt{F_+^2-A^2}-F_-\sqrt{F_+^2-A^2}}{(F_+^2-A^2)^{3/2}} + \frac{A^2}{(F_+^2-A^2)^{3/2}}\ln\left(\frac{\sqrt{F_-^2-A^2}+F_-}{\sqrt{F_+^2-A^2}+F_+}\right) \right. \\
& \left. \left. + \frac{(F_-^2-A^2)^{3/2}}{F_-(F_+^2-A^2)^{3/2}} - \frac{1}{F_+}\right] e^{\phi_1(1-\Gamma)}\right\}, \\
C_4' = & \left[-\frac{F_-^2-A^2}{F_+^2-A^2} - e^{(\phi_1+\phi_2)(1-\Gamma)}\right]^{-1} \left\{ \frac{\sqrt{F_+^2-A^2}(F_-^2-A^2)}{F_+} \right. \\
& + \frac{F_-^2-A^2}{F_+^2-A^2}\left[F_+\sqrt{F_+^2-A^2} - A^2\ln\left(\frac{\sqrt{F_+^2-A^2}+F_+}{A}\right)\right] + e^{\phi_2(1-\Gamma)} \\
& \times \left[-\frac{(F_-^2-A^2)^{3/2}}{F_-} + \frac{\sqrt{F_+^2-A^2}(F_-^2-A^2)}{F_+}\right] - e^{(\phi_1+\phi_2)(1-\Gamma)} \\
& \left. \times \left[F_-\sqrt{F_-^2-A^2} - A^2\ln\left(\frac{\sqrt{F_-^2-A^2}+F_-}{A}\right) - \frac{(F_-^2-A^2)^{3/2}}{F_-}\right]\right\}.
\end{aligned}
\tag{A.8}
$$

For $F_- < A < F_+$, the probability density is expressed as

$$P(y) = \begin{cases} \dfrac{\langle \dot{y} \rangle}{L} \left(D_1 \, e^{2\phi_1 y/L} - \dfrac{1}{F_-} \right) & \text{for } y \in [0, L/2 - 2l) \\ \dfrac{\langle \dot{y} \rangle}{L} \dfrac{D_2}{\sqrt{A^2 - F^2(y)}} & \text{for } y \in [L/2 - 2l, y_1) \\ \dfrac{\langle \dot{y} \rangle}{L} \dfrac{D_3}{\sqrt{F^2(y) - A^2}} & \text{for } y \in (y_1, L/2) \\ \dfrac{\langle \dot{y} \rangle}{L} \left[D_4 \, e^{2\phi_2 (y/L - 1/2)} - \dfrac{1}{F_+} \right] & \text{for } y \in [L/2, L - 2l) \\ \dfrac{\langle \dot{y} \rangle}{L} \left\{ \dfrac{F(y)}{[F^2(y) - A^2]} \right. & \\ \quad \left. + \dfrac{A^2 \ln \left\{ \left[\sqrt{F^2(y) - A^2} - F(y) \right] / A \right\}}{[F^2(y) - A^2]^{3/2}} \right\} & \text{for } y \in [L - 2l, y_2) \\ \dfrac{\langle \dot{y} \rangle}{L} \left\{ \dfrac{-F(y)}{[A^2 - F^2(y)]} \right. & \\ \quad \left. + \dfrac{-A^2 \left[\pi/2 + A^2 \arcsin[F(y)/A] \right]}{[A^2 - F^2(y)]^{3/2}} \right\} & \text{for } y \in (y_2, L) \end{cases} \tag{A.9}$$

and the mean drift velocity as

$$\begin{aligned} \langle \dot{x} \rangle = & v + \left\{ D_1 \frac{e^{\phi_1 (1-\Gamma)} - 1}{2\phi_1} + D_4 \frac{e^{\phi_2 (1-\Gamma)} - 1}{2\phi_2} - \frac{v(1-\Gamma)}{F_+ F_-} \right. \\ & + \frac{\Gamma}{4bv} \left[\left(D_2 + \frac{F_-}{\sqrt{A^2 - F_-^2}} \right) (\pi/2 - \arcsin(F_-/A)) \right. \\ & \left. \left. + \left(D_3 - \frac{F_+}{\sqrt{F_+^2 - A^2}} \right) \ln \left(\frac{\sqrt{F_+^2 - A^2} + F_+}{A} \right) \right] \right\}^{-1} \end{aligned} \tag{A.10}$$

where the integration constants D_1–D_4 are given by

$$\begin{aligned} D_1 = & \frac{1}{F_-} + \frac{F_- \sqrt{A^2 - F_-^2} + A^2 \arcsin(F_-/A) - A^2 \pi/2}{\left(A^2 - F_-^2 \right)^{3/2}}, \\ D_2 = & \frac{\sqrt{A^2 - F_-^2} \left[e^{\phi_1 (1-\Gamma)} - 1 \right]}{F_-} \\ & + e^{\phi_1 (1-\Gamma)} \left[\frac{F_- \sqrt{A^2 - F_-^2} + A^2 \arcsin(F_-/A) - A^2 \pi/2}{A^2 - F_-^2} \right], \end{aligned}$$

$$
\begin{aligned}
D_3 =& \frac{\sqrt{F_+^2 - A^2}\left[e^{-\phi_2(1-\Gamma)} - 1\right]}{F_+} \\
&+ e^{-\phi_2(1-\Gamma)} \left\{ \frac{A^2 \ln\left[\left(\sqrt{F_+^2 - A^2} + F_+\right)/A\right] - F_+\sqrt{F_+^2 - A^2}}{F_+^2 - A^2} \right\}, \\
D_4 =& e^{-\phi_2(1-\Gamma)} \left\{ \frac{1}{F_+} \right. \\
&\left. + \frac{A^2 \ln\left[\left(\sqrt{F_+^2 - A^2} + F_+\right)/A\right] - F_+\sqrt{F_+^2 - A^2}}{\left(F_+^2 - A^2\right)^{3/2}} \right\}.
\end{aligned} \tag{A.11}
$$

Appendix B. The Problem of Hypersensitive Transport: Particular Cases for the Piecewise Linear Velocity Profile

Again, explicit results can be obtained for the case $\alpha = 1/2$. When there are no fixed points one obtains for the probability density:

$$
P(x) = \begin{cases}
\dfrac{\langle \dot{x} \rangle}{LF} \left\{ 1 + \dfrac{2f\Delta \arcsin(1/f)}{(\Delta+1)(f+1)^{3/2}\sqrt{f-1}} \right. & \\
\qquad \left. \times \exp\left[-\dfrac{4f}{(f^2-1)\Gamma} \dfrac{x}{L} \right] \right\} & \text{for } x \in [0, L/2 - 2l) \\
\dfrac{\langle \dot{x} \rangle}{LF} \left\{ 1 + \dfrac{\chi}{(f-\chi)^{3/2}\sqrt{f+\chi}} \right. & \\
\qquad \times \left\{ \sqrt{f^2-\chi^2} - \sqrt{f^2-1} \right. & \text{for } x \in [L/2 - 2l, L/2) \\
\qquad \left. \left. + f \arcsin(\chi/f) - f\dfrac{\Delta-1}{\Delta+1} \arcsin(1/f) \right\} \right\} &
\end{cases} \tag{B.12}
$$

where $\chi = 2\Gamma - 1 - x/l$. The mean velocity is

$$
\frac{\langle \dot{x} \rangle}{F} = \left\{ 1 - 2\Gamma + 2\Gamma\sqrt{f^2-1}\, \arcsin\left(\frac{1}{f}\right) + \frac{\Gamma f(\Delta-1)}{\Delta+1} \left[\arcsin\left(\frac{1}{f}\right) \right]^2 \right\}^{-1}, \tag{B.13}
$$

where

$$
\Delta = \left(\frac{f+1}{f-1}\right) \exp\left[\frac{2f(1-\Gamma)}{(f^2-1)\Gamma} \right]. \tag{B.14}
$$

When there are two fixed points, $P(x)$ has an integrable power-law singularity

at the stable fixed point:

$$P(x) = \begin{cases} \dfrac{\langle \dot{x} \rangle}{LF} \left\{ 1 + \exp\left[\dfrac{4f}{\Gamma(1-f^2)} \left(\dfrac{x}{L} - \dfrac{1-\Gamma}{2} \right) \right] \right. & \\ \qquad \left. \times \dfrac{f \ln\left[(1+\sqrt{1-f^2})/f \right] - \sqrt{1-f^2}}{(1-f)^{3/2}\sqrt{1+f}} \right\} & \text{for } x \in [0, L/2 - 2l) \\ \dfrac{\langle \dot{x} \rangle}{LF} \left\{ 1 + \dfrac{\chi}{(\chi - f)^{3/2}\sqrt{\chi + f}} \right. & \\ \qquad \left. \times \left\{ f \ln\left[\dfrac{\chi + \sqrt{\chi^2 - f^2}}{f} \right] - \sqrt{\chi^2 - f^2} \right\} \right\} & \text{for } x \in [L/2 - 2l, x_1) \\ \dfrac{\langle \dot{x} \rangle}{LF} \left\{ 1 + \dfrac{\chi}{(f - \chi)^{3/2}\sqrt{\chi + f}} \right. & \\ \qquad \left. \times \left\{ \sqrt{f^2 - \chi^2} + f \left[\arcsin\left(\dfrac{\chi}{f} \right) - \dfrac{\pi}{2} \right] \right\} \right\} & \text{for } x \in (x_1, x_2) \\ \dfrac{\langle \dot{x} \rangle}{LF} \left\{ 1 + \dfrac{\chi}{(f - \chi)^{3/2}(-\chi - f)^{1/2}} \right. & \\ \qquad \left\{ \sqrt{\chi^2 - f^2} \right. & \\ \qquad - \sqrt{1-f^2} + f \ln\left[\dfrac{\sqrt{\chi^2 - f^2} - \chi)}{\sqrt{1-f^2} + 1} \right] & \\ \qquad - \exp\left(-\dfrac{2f(1-\Gamma)}{\Gamma(1-f^2)} \right) \left(\dfrac{1+f}{1-f} \right) & \text{for } x \in (x_2, L/2). \\ \qquad \left. \left. \times \left[f \ln\left(\dfrac{1+\sqrt{1-f^2}}{f} \right) - \sqrt{1-f^2} \right] \right\} \right\} & \end{cases} \tag{B.15}$$

For the mean velocity we find

$$\begin{aligned}\frac{\langle\dot{x}\rangle}{F} = &\left\{1+\Gamma\left[f\frac{\pi^2}{4}+\frac{f}{2}-\frac{3}{2}+\frac{1+f}{2}\exp\left(-\frac{2f(1-\Gamma)}{\Gamma(1-f^2)}\right)\right]\right.\\ &+\left[1-\exp\left(-\frac{2f(1-\Gamma)}{\Gamma(1-f^2)}\right)\right]\frac{\Gamma\sqrt{1+f}}{2f\sqrt{1-f}}\\ &\times\left[f\ln\left(\frac{1+\sqrt{1-f^2}}{f}\right)-\sqrt{1-f^2}\right]\\ &+\frac{\Gamma f}{2}\ln^2\left(\frac{1+\sqrt{1-f^2}}{f}\right)\left[1+\frac{1+f}{1-f}\exp\left(-\frac{2f(1-\Gamma)}{\Gamma(1-f^2)}\right)\right]\\ &+\frac{\Gamma}{2}\ln\left(\frac{1+\sqrt{1-f^2}}{f}\right)\left[\sqrt{\frac{1-f}{1+f}}-\frac{2f^2}{\sqrt{1-f^2}}\right.\\ &\left.\left.-\ (1+2f)\sqrt{\frac{1+f}{1-f}}\exp\left(-\frac{2f(1-\Gamma)}{\Gamma(1-f^2)}\right)\right]\right\}^{-1}.\end{aligned} \tag{B.16}$$

Acknowledgments

This work was partially supported by the Swiss National Science Foundation (I.B.) and by the National Science Foundation under grant Nos. PHY-0354937.

References

[1] F. Moss and P. V. E. McClintock, eds., *Noise in Nonlinear Dynamical Systems*, Cambridge University Press, Cambridge (1989); K. Lindenberg, B. J. West, and G. P. Tsironis, *Bistable systems driven by colored noise*, *Rev. Solid State Sci.* **3** (1989) 143; K. Lindenberg and B. J. West, *The Nonequilibrium Statistical Mechanics of Open and Closed Systems*, VCH Publishers, New York (1990); P. Hänggi and P. Jung, *Colored noise in dynamical systems*, *Advances in Chemical Physics* **LXXXIX** (1995),239.

[2] J. M. Sancho, *External dichotomous noise: The problem of the mean-first-passage time*, *Phys. Rev. A* **31** (1985) 3523; J. Masoliver, K. Lindenberg, and B. J. West, *First-passage times for non-Markovian processes*, *Phys. Rev. A* **33** (1986) 2177; J. Masoliver, K. Lindenberg, and B. J. West, *First-passage times for non-Markovian processes: Correlated impacts on a free process*, *Phys. Rev. A* **34** (1986) 1481; J. Masoliver, K. Lindenberg, and B. J. West, *First-passage times for non-Markovian processes: Correlated impacts on bound processes*, *Phys. Rev. A* (1986) 2351; M. A. Rodriguez and L. Pesquera, *First-passage times for non-Markovian processes driven by dichotomic Markov noise*, *Phys. Rev. A* **34** (1986) 4532; C. R. Doering, *Comment on first-passage times for processes driven by dichotomous fluctuations*, *Phys. Rev. A* **35** (1987) 3166; V. Balakrishnan, C. Van den Broeck, and P. Hänggi, *First-passage times of non-Markovian processes: The case of a reflecting boundary*, *Phys. Rev. A* **38** (1988) 4213; U. Behn and K. Schiele, *Stratonovich model driven by dichotomous noise: Mean first passage time*, *Z. Phys. B* **77** (1989) 485; M. Kuś, E. Wajnryb and K. Wódkiewicz, *Mean first-passage time in the presence of colored noise: A random-telegraph-signal approach*, *Phys. Rev. A* **43** (1991) 4167; J. Olarrea, J. M. R.

Parrondo, and F. J. de la Rubia, *Escape statistics for systems driven by dichotomous noise. I. General theory*, *J. Stat. Phys.* **79** (1995) 683; J. Olarrea, J. M. R. Parrondo, and F. J. de la Rubia, *Escape statistics for systems driven by dichotomous noise. II. The imperfect pitchfork bifurcation as a case study*, *J. Stat. Phys.* **79** (1995) 669; C. Doering, W. Horsthemke, and J. Riordan, *Nonequilibrium fluctuation-induced transport*, *Phys. Rev. Lett.* **72** (1994) 2984.

[3] S. Mangioni, R. R. Deza, H. S. Wio, and Toral, *Disordering effects of color in nonequilibrium phase transitions induced by multiplicative noise*, *Phys. Rev. Lett.* **79** (1997) 2389.

[4] S. E. Mangioni, R. R. Deza, R. Toral, and H. S. Wio, *Nonequilibrium phase transitions induced by multiplicative noise: Effects of self-correlation*, *Phys. Rev. E* **61** (2000) 223.

[5] Y. Kim and W. Sung, *Does stochastic resonance occur in periodic potentials?*, *Phys. Rev. E* **57** (1998) 6237(R).

[6] R. Rozenfeld, A. Neiman, and L. Schimansky-Geier, *Stochastic resonance enhanced by dichotomic noise in a bistable system*, *Phys. Rev. E* **62** (2000) 3031(R).

[7] R. Rozenfeld, J. A. Freund, A. Neiman, and L. Schimansky-Geier, *Noise-induced phase synchronization enhanced by dichotomic noise*, *Phys. Rev. E* **64** (2001) 051107.

[8] N. G. Van Kampen, *Stochastic Processes in Physics and Chemistry*, North-Holland, Amsterdam (1992).

[9] I. Bena, C. Van den Broeck, R. Kawai, and K. Lindenberg, *Nonlinear response with dichotomous noise*, *Phys. Rev. E* **66** (2002) 045603(R).

[10] I. Bena, C. Van den Broeck, R. Kawai, and K. Lindenberg, *Drift by dichotomous Markov noise*, *Phys. Rev. E* **68** (2003) 041111.

[11] I. Bena, M. Copelli, and C. Van den Broeck, *Stokes' drift: A rocking ratchet*, *J. Stat. Phys.* **101** (2000) 415.

[12] M. B. Tarlie and R. D. Astumian, *Optimal modulation of a Brownian ratchet and enhanced sensitivity to a weak external force*, *Proc. Natl. Acad. Sci. USA* **95** (1998), 2039; V. Berdichevsky and M. Gitterman, *Stochastic resonance and ratchets - new manifestations*, *Physica A* **249** (1998) 88; S. L. Ginzburg and M. A. Pustovoit, *Hypersensitive transport in a phase model with multiplicative stimulus*, *Phys. Lett. A* **291** (2001) 77; *ibid*, *Noise-induced hypersensitivity to small time-dependent signals*, *Phys. Rev. Lett.* **80** (1998) 4840; *ibid*, *Hypersensitivity of a nonlinear system with multiplicative colored noise to an external periodic system*, *J. Exp. Th. Phys.* **89** (1999) 801; *ibid.*, *Stochastic resonance, on-off intermittency and "physical mathematics"* *Europhys. Lett.* **45** (1999), 540; O. V. Gerashchenko, S. L. Ginzburg, and M. A. Pustovoit, *Hypersensitivity to small signals in a stochastic system with multiplicative colored noise*, *Eur. Phys. J. B* **19** (2001) 101; R. Mankin, A. Haljas, R. Tammelo, and D. Martila, *Mechanism of hypersensitive transport in tilted sharp ratchets*, *Phys. Rev. E* **68** (2003), 011105.

[13] O. V. Gerashchenko, S. L. Ginzburg, and M. A. Pustovoit, *Multiplicative-noise-induced amplification of weak signals in a system with on-off intermittency*, *J. Exp. Theor. Phys. Lett.* **67**, (1998), 997; *ibid.*, *Experimental observation of noise-induced sensitivity to small signals in a system with on-off intermittency*, *Eur. J. Phys. B* **15** (2000), 335; S. L. Ginzburg and M. A. Pustovoit, *Stochastic resonance in two-state model of membrane channel with comparable opening and closing rates*, *Phys. Rev. E* **66** (2002), 021107; *ibid.*, *Bursting dynamics of a model neuron induced by intrinsic channel noise*, *Fluct. Noise Lett.* **3** (2003) L265.

[14] A few recent papers from a rich bibliography on the subject include: A. M. Bratseth, *On the estimation of transport characteristics of atmospheric data sets*, *Tellus* **50A**

(1998) 451; S. M. Cox, *Onset of Langmuir circulation when shear flow and Stokes drift are not parallel*, *Fluid Dyn. Res.* **19** (1997) 149; H. C. Graber, B. K. Haus, R. D. Chapman and L. K. Shay, *HF Radar comparisons with moored estimates of current speed and direction: Expected differences and implications*, *J. Geophys. Res. - Oceans* **102** (1997) 18749; J. C. McWilliams, P. P. Sullivan and Chin-Hoh Moeng, *Langmuir turbulence in the ocean*, *J. Fluid Mech.* **334** (1997) 1; M. Nordsveen and A. F. Bertelsen, *Wave induced secondary motions in stratified duct flow*, Int. J. Multiphase Flow **23** (1997) 503; V. Polonichko, *Generation of Langmuir circulation for nonaligned wind stress and the Stokes drift*, *J. Geophys. Res.* **102** (1997) 15773; S. A. Thorpe, *Interactions between internal waves and boundary layer vortices*, *J. Phys. Oceanogr.* **27** (1997) 62; *ibid.*, *On the interactions of internal waves reflecting from slopes*, (1997) 2072.

[15] See e.g. C. P. Lee, *The balancing of thermocapillary flow in a floating zone by ripple-driven streaming*, *Phys. of Fluids* **10** (1998) 2765 and references therein.

[16] C. Van den Broeck, *Stokes' drift: An exact result*, *Europhys. Lett.* **46** (1999) 1.

[17] K. Herterich and K. Hasselmann, *The horizontal diffusion of tracers by surface waves*, *J. Phys. Oceanogr.* **12** (1982) 704; O. N. Mesquita, S. Kane and J. P. Gollub, *Transport by capillary waves: Fluctuating Stokes drift*, *Phys. Rev. A* **45** (1992) 3700; K. M. Janson and G. D. Lythe, *Stochastic Stokes drift*, *Phys. Rev. Lett.* **81** (1998) 3136; ibid., *Stochastic calculus: Application to dynamic bifurcations and threshold crossings*, *J. Stat. Phys.* **90** (1998) 227; R. Landauer and M. Büttiker, *Drift and diffusion in reversible computation*, *Physica Scripta* **T9** (1985) 155.

[18] For an overview, see P. Reimann, *Brownian motors: noisy transport far from equilibrium*, Phys. Rep. **361** (2002) 57 and references therein.

[19] F. Marchesoni and M. Borromeo, *Stokes drift of linear defects*, *Phys. Rev. B* **65** (2002) 184101.

[20] C.R. Doering, W. Horsthemke and J. Riordan, *Nonequilibrium fluctuation-induced transport*, *Phys. Rev. Lett.* **72** (1994) 2984; K. W. Kehr, K. Mussawisade, T. Wichmann and W. Dieterich, *Rectification by hopping motion through nonsymmetric potentials with strong bias*, *Phys. Rev. E* **56** (1997) R2351.

[21] The half delta functions are defined as

$$\lim_{\varepsilon\searrow 0}\int_{-\infty}^{-\varepsilon}\delta_-(x)f(x)dx = (1/2)\lim_{x\nearrow 0} f(x) = (1/2)f(-0)$$
$$\lim_{\varepsilon\searrow 0}\int_{+\varepsilon}^{+\infty}\delta_-(x)f(x)dx = 0$$
$$\lim_{\varepsilon\searrow 0}\int_{-\infty}^{-\varepsilon}\delta_+(x)f(x)dx = 0$$
$$\lim_{\varepsilon\searrow 0}\int_{+\varepsilon}^{+\infty}\delta_+(x)f(x)dx = (1/2)\lim_{x\searrow 0} f(x) = (1/2)f(+0)$$

with $\delta(x) = \delta_-(x) + \delta_+(x)$.